Rapid and rigorous 3D inversion of airborne electromagnetic data

Leif H. Cox and Michael S. Zhdanov, University of Utah*

SUMMARY

We address the challenging problem of interpreting frequency domain helicopter-borne electromagnetic data in areas with rough topography. Our method is based on localized quasi-linear (LQL) inversion followed by rigorous inversion, if necessary. Terrain corrections are also included. The LQL inversion serves to provide a fast image of the target. These results are checked by rigorous successive iterations of the domain equation, allowing more accurate calculation of the predicted data. If the accuracy is poorer than desired, rigorous inversion follows, using the LQL result as a starting model. We test this method on synthetic data and field data using the new code LQLRigInvTOPO. The results of the inversion are very encouraging with respect to both the speed and the accuracy of the algorithm. The numerical study shows that the new code with terrain correction provides a useful tool for airborne EM interpretation.

INTRODUCTION

One of the most challenging problems in mineral exploration is interpretation of airborne EM data over 3D geoelectrical targets. Over the last several years, the Consortium for Electromagnetic Modeling and Inversion (CEMI) has developed methods and the corresponding software for a solution of this problem based on the localized quasi-linear (LQL) approximation (Zhdanov and Tartaras, 2002; Katayama and Zhdanov, 2004). This method provides a fast algorithm for 3D imaging of conductive targets. It can be treated as an effective reconnaissance tool, or accurate inversion in the case of simple target geometry and low conductivity contrasts. However, when these conditions are not met, the recovered conductivity of the target may be significantly underestimated, and the shape of the inverse images may be distorted in comparison with the true model.

In the current paper, we attempt to overcome this limitation of the LQL method by considering a rigorous forward modeling technique in the framework of the regularized inversion scheme. According to this approach, the solution of the helicopter EM (HEM) inverse problem is formulated using two sets of integral equations: 1) a field equation connecting the observed data in the receivers with the anomalous conductivity within the inversion domain; 2) a domain equation with respect to the electric field inside the anomalous domain. The main difficulty in the solution of these equations arises from the fact that, in the case of the HEM survey, we are dealing with multi-transmitter, multi-receiver data. This requires simultaneous analysis of as many pairs of the field and domain equations as we have transmitter positions. We use a contraction form of the domain equation to ensure convergence of the iterative inversion.

It is important to emphasize that this technique can take into account the effect of rough topography as well (Katayama and Zhdanov, 2004). It turns out that topography can be modeled by the presence of a near-surface anomalous body with a strong conductivity contrast. This is why rough topography can significantly distort EM data, resulting in erroneous interpretations. Therefore, this effect should be taken into account when interpretating airborne EM data.

In this paper, we develop a new fast and rigorous 3D inversion technique for airborne EM data which takes into account the distortion caused by the rough earth-air interface and compensates the inversion results for topographic effects.

INVERSION ALGORITHM

In this section, we outline a method for inverting frequency domain HEM data. This type of airborne survey is used extensively in mineral exploration. We consider a 3D geoelectrical model with a background (horizontally layered) conductivity, σ_b, and a local inhomogeneity, D, with an arbitrarily varying conductivity, $\sigma = \sigma_b + \Delta\sigma$. In the framework of the HEM method, one uses a moving transmitter-receiver system consisting of a pair of vertical magnetic dipoles (a horizontal coplanar coil pair) and a pair of horizontal magnetic dipoles (a vertical coaxial coil pair). A frequency domain EM field is generated by a transmitter dipole and is recorded by a receiver dipole. The goal is to find the anomalous conductivity distribution, $\Delta\sigma$, based on the data collected by the HEM survey.

According to the integral form of Maxwell's equations, the anomalous field in the frequency domain can be represented as an integral over the excess (anomalous) currents, $\mathbf{j}^a = \Delta\sigma\mathbf{E}$, in the inhomogeneous domain D :

$$\mathbf{E}^a\left(\mathbf{r}_j\right) = \mathbf{G}_E\left(\Delta\sigma\mathbf{E}\right) = \iiint_D \widehat{\mathbf{G}}_E\left(\mathbf{r}_j \mid \mathbf{r}\right)\Delta\sigma\left(\mathbf{r}\right)\mathbf{E}\left(\mathbf{r}\right)dv, \tag{1}$$

$$\mathbf{H}^a\left(\mathbf{r}_j\right) = \mathbf{G}_H\left(\Delta\sigma\mathbf{E}\right) = \iiint_D \widehat{\mathbf{G}}_H\left(\mathbf{r}_j \mid \mathbf{r}\right)\Delta\sigma\left(\mathbf{r}\right)\mathbf{E}\left(\mathbf{r}\right)dv, \tag{2}$$

where $\widehat{\mathbf{G}}_{E,H}\left(\mathbf{r}_j \mid \mathbf{r}\right)$ stands for the electric or magnetic Green's tensor defined for an unbounded conductive medium with normal conductivity, σ_b.

Equation (2), which connects the observed magnetic field at the receivers with the electric field inside the anomalous domain, D, represents *a field equation*. Writing equation (1) for the points within the anomalous domain, $\mathbf{r}_j \in D$, we arrive at *a domain equation*.

Following Gribenko and Zhdanov (2005), we first solve the HEM inverse problem using the localized quasi-linear (LQL) method (Zhdanov and Tartaras, 2002). This method is based on the assumption that the anomalous field, $\mathbf{E}^a$, inside the inhomogeneous domain is linearly proportional to the background field, $\mathbf{E}^b$, through electrical reflectivity tensor, $\widehat{\lambda}$, (Zhdanov and Fang, 1996a,b), which is assumed to be independent of the transmitter position:

$$\mathbf{E}^a\left(\mathbf{r}\right) \approx \widehat{\lambda}\left(\mathbf{r}\right)\cdot\mathbf{E}^b\left(\mathbf{r}\right). \tag{3}$$

We denote the anomalous conductivity obtained by the LQL inversion as $\Delta\sigma_{LQL}$.

The rigorous stage of the inversion is based on the iterative solution of the field and domain equations. However, in order to ensure the convergence of the corresponding iterative process, we use the contraction form of the domain equation Hursán and Zhdanov (2002):

$$a\mathbf{E}^a + b\mathbf{E}^b = \mathbf{G}_E^m\left[b(\mathbf{E}^a + \mathbf{E}^b)\right], \tag{4}$$

where

$$a = \frac{2\sigma_b + \Delta\sigma}{2\sqrt{\sigma_b}},\ b = \frac{\Delta\sigma}{2\sqrt{\sigma_b}}, \tag{5}$$

and modified Green's operator $\mathbf{G}_E^m\left(\mathbf{x}\right)$ is defined as a linear transformation of the original electric Green's operator:

$$\mathbf{G}_E^m\left(\mathbf{x}\right) = \sqrt{\sigma_b}\mathbf{G}_E\left(2\sqrt{\sigma_b}\mathbf{x}\right) + \mathbf{x}. \tag{6}$$

The advantage of equation (4) over the conventional domain equation is that the L_2 norm of the modified Green's operator is always less than or equal to one, $\|\mathbf{G}_E^m\| \leq 1$.

The electric field computed for the given reflectivity tensor and conductivity inside domain D for the transmitter position with the index I is denoted by $\mathbf{E}_I^{(0)}(\mathbf{r})$.

Let $\mathbf{H}_I^{pr(LQL)}(\mathbf{r}_j)$ denote the predicted anomalous magnetic field in the receivers computed for the conductivity model $\Delta\sigma_{LQL}(\mathbf{r})$:

$$\mathbf{H}_I^{pr(LQL)}(\mathbf{r}_j) = \mathbf{G}_H\left[\Delta\sigma_{LQL}\mathbf{E}_I^{(0)}\right]. \tag{7}$$

Note that the Green's operator, $\mathbf{G}_H$, is the same as in formula (2). It acts from the point $\mathbf{r}$ inside domain D to the receiver position $\mathbf{r}_j$. We can estimate now how accurate our LQL inversion is by computing the normalized error of the LQL approximation, ε_{LQL}:

$$\varepsilon_{LQL} = \frac{\left\|\mathbf{H}_I^{pr(LQL)}(\mathbf{r}_j) - \mathbf{H}_I^a(\mathbf{r}_j)\right\|}{\left\|\mathbf{H}_I^a(\mathbf{r}_j)\right\|}. \tag{8}$$

We finish the inverse process if the error of the LQL inversion is less than the given accuracy level ε_0, $\varepsilon_{LQL} \leq \varepsilon_0$. Otherwise we can apply the LQL inversion iteratively.

On each iteration we use the updated field, $\mathbf{E}_I^{(k-1)}(\mathbf{r})$, to find an updated conductivity $\Delta\sigma^{(k)}(\mathbf{r})$ from the equation:

$$\mathbf{H}_I^a(\mathbf{r}_j) = \iiint_D \widehat{\mathbf{G}}_H(\mathbf{r}_j \mid \mathbf{r}) \cdot \Delta\sigma^{(k)}(\mathbf{r})\mathbf{E}_I^{(k-1)}(\mathbf{r})\,dv$$

$$= \mathbf{G}_H\left[\Delta\sigma^{(k)}\mathbf{E}_I^{(k-1)}\right],\ I = 1,2,\ldots N. \tag{9}$$

We solve inverse problem (9) using the regularized reweighted conjugate gradient method (Zhdanov, 2002).

We update the electric field $\mathbf{E}^{(k)}(\mathbf{r})$ using the integral expression:

$$\mathbf{E}_I^{(k)}(\mathbf{r}') =$$

$$\frac{b\mathbf{E}^{(k-1)} + 2\sqrt{\sigma_b}\mathbf{G}_E[\sqrt{\sigma_b}b\mathbf{E}^{(k-1)}] + \sqrt{\sigma_b}\mathbf{E}^b}{a},\ I = 1,2,\ldots N. \tag{10}$$

where parameters a and b are updated from the new $\Delta\sigma$.

Note that one iteration of equation (10) is usually sufficient to obtain an accurate estimate to the electric field from $\Delta\sigma^{(k)}$, so this process is relatively fast. In addition, as the inversion converges the change in $\Delta\sigma$ on each iteration becomes smaller, allowing for a very accurate electric field. To ensure convergence in the initial stages when the true electric field may be far from the initial guess, we can iterate several times over equation (10) until the error in the electric field becomes small.

For the model with conductivity $\Delta\sigma^{(k)}(\mathbf{r})$, we can calculate the predicted anomalous magnetic field $\mathbf{H}_I^{pr(1)}(\mathbf{r}_j)$ based on the equation:

$$\mathbf{H}_I^{pr(k)}(\mathbf{r}_j) = \iiint_D \widehat{\mathbf{G}}_H(\mathbf{r}_j \mid \mathbf{r}) \cdot \Delta\sigma^{(k)}(\mathbf{r})\mathbf{E}_I^{(k)}(\mathbf{r})\,dv =$$

$$= \mathbf{G}_H\left[\Delta\sigma^{(k)}\mathbf{E}_I^{(k)}\right]. \tag{11}$$

We also can estimate the accuracy of this solution by computing the normalized error of the inversion:

$$\varepsilon_k = \frac{\left\|\mathbf{H}_I^{pr(k)}(\mathbf{r}_j) - \mathbf{H}_I^a(\mathbf{r}_j)\right\|}{\left\|\mathbf{H}_I^a(\mathbf{r}_j)\right\|}.$$

The iterative process continues until we reach the required level of misfit.

INVERSION TESTING

Synthetic Body

We first test the algorithm on synthetic data. The model is modified from Zhang (2003); it contains two bodies at different depths with different resistivities. Forty-eight data points were synthesized for each of 3 channels along 6 flight lines as shown in Figure 1(a) over the displayed body. Topography was included in the forward model as a ridge 200 m wide with a maximum elevation of 25 m. The strike extends from y=0 m to y=600 m. The upper body is 10 Ωm and the lower body is 2 Ωm; they are imbedded in a 100 Ωm halfspace.

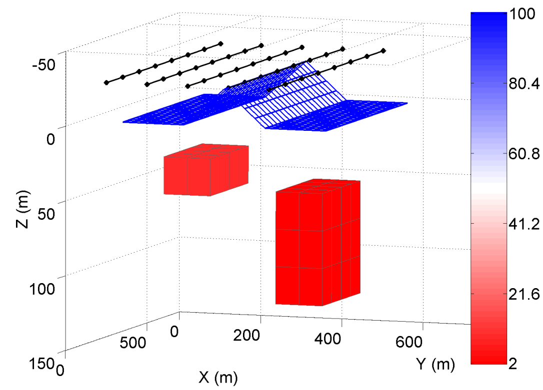

(a)

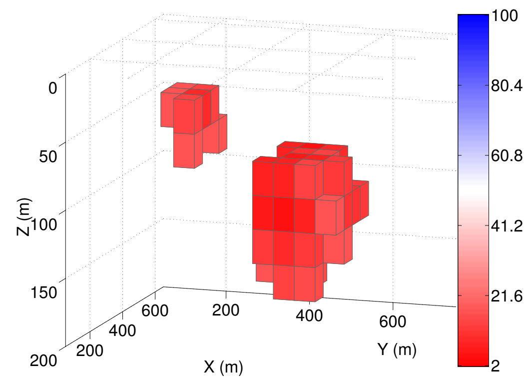

(b)

Figure 1: Inversion results given in total resistivity (Ωm). Shown are the true body, topography, and survey layout (a) and the inversion result (b). The resistivity cutoff for the 3D view is 18 Ωm.

The three channels used for inversion (900 Hz Coplanar, 900 Hz Coaxial, and 7200 Hz Coplanar) were contaminated with 6% noise. The rigorous inversion was run to 20% misfit, as shown in Figure 3. The observed and predicted data with terrain effects for the 7200 Hz channel is shown in Figure 2(a). Note that the response from the bodies is almost completely obscured by the terrain. For comparison, we also show the observed and predicted data for all channels in Figure 2(b). The result of the inversion using all three channels is displayed in Figure 1(b). The effects of the terrain have been completely removed from the inversion result, as shown by the accurate delineation of both the location and conductivity of both bodies.

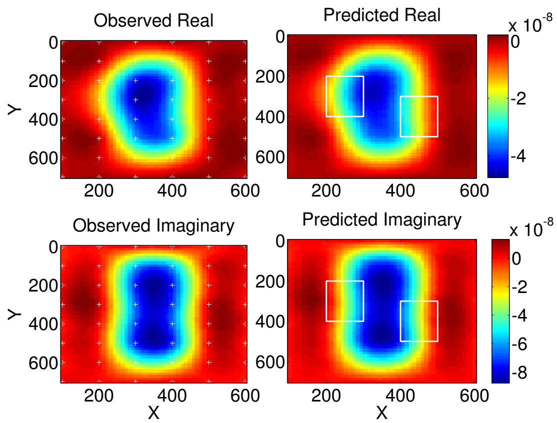

(a)

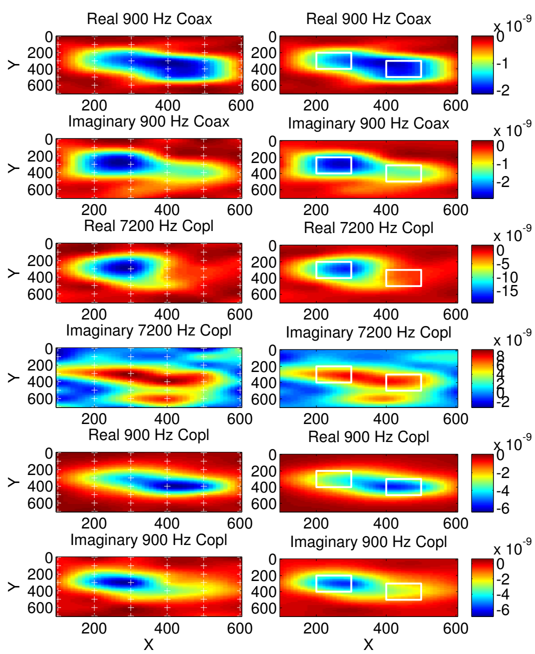

(b)

Figure 2: Observed data and predicted anomalous data from the 7200 Hz Channel, including the effect of the ridge (a) and observed and predicted anomalous data from the inversion with the terrain effects removed. It is apparent one need to compensate for the terrain to obtain accurate inversion. Data points are shown as white crosses and the body locations are shown as the white boxes. The observed data are shown on the left, and the predicted data are shown on the right. The colorbar units are A/m.

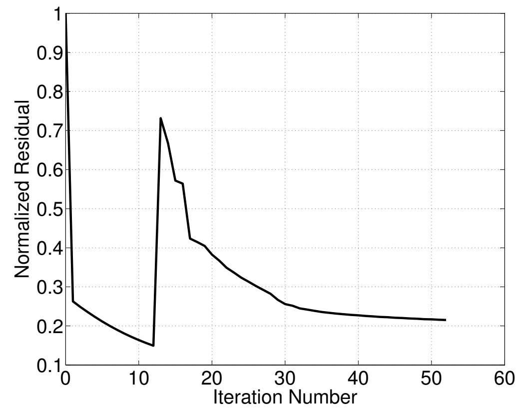

Figure 3: Normalized residual versus iteration number. LQL inversion runs for 10 iterations. The final predicted misfit from LQL is 15%, but the rigorous check shows the true error in the solution to be 77%. The rigorous inversion then runs to 20% error.

Frequency (Hz)	Component
871	Coplanar
1095	Coaxial
5834	Coaxial
7166	Coplanar
55590	Coplanar

Table 1: DIGHEM data over the kimberlite pipe.

Inversion of HEM over a Kimberlite Pipe

Geologic Setting

The survey data we have applied our inversion algorithm to is from the Ekati Diamond Mine, Canada. The data were graciously provided by BHP Billiton Diamonds, Inc. The target is a kimberlite pipe, which is the main diamond bearing ore. Kimberlite pipes are an ultrabasic intrusion which are nearly circular and narrow with depth. The kimberlite material typically weathers more rapidly into clays, which provides a conductive target for EM methods (Macnae, 1979). The location in question has been glacially scoured, which has preferentially removed part of the weathered clay cap and left in its wake a lake. The lake bottom has significant bathymetric relief which we include as a priori information to test the terrain correction part of the code.

Survey and Inversion Parameters

This survey was performed with the DIGHEM system consisting of 5 channels (Table 1). We selected the 3 coplanar components for the test of our inversion code. The original survey had very dense measurements, but for our inversion we used only every 50th data point giving a total of 68 measurements for each channel. The flight height was approximately 25 meters above the lake, and the transmitter-receiver separation was 7 m.

The inversion domain contained 2700 cells; 15 in the x and y directions and 12 in the z direction, all linearly spaced. The inversion domain extended from 118 m to 1030 m in the x, 437 m to 1440 m in the y, and 0 m to 500 m in the z direction.

First, a 1D inversion was performed to find a layered earth background model. The results for the layered earth background model are shown in Table 2. This model was used for the 3D inversion scheme, as out-

Layer	Conductivity (S/m)	Base Depth (m)
Water	0.00016	5-35
1	0.00055	38.5
2	0.0035	82.5
3	0.0030	Inf

Table 2: One dimensional layered earth model.

lined above. The final misfit in the predicted data from LQL after 10 iterations is 25%, but the true error in the solution as rigorously calculated using the scheme above is 77%.

We then use the LQL result as a starting model and followed the rigorous inversion algorithm to further delineate the model. The rigorous inversion runs for an additional 40 iterations giving a final rigorous misfit of 39%. The results from this stage of inversion are shown in Figure 4. The total inversion time on a 2.4 GHz AMD 64 processor with 4 Gb of RAM was 45 minutes. The maximum ram used was 600 Mb.

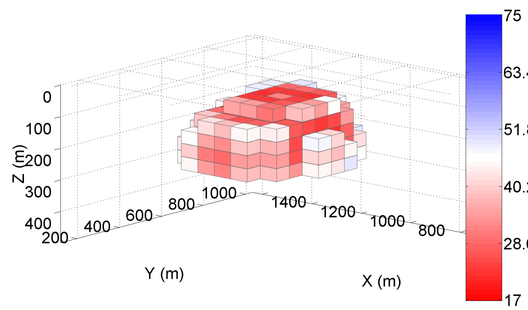

Figure 4: Inversion results are given in total resistivity (Ωm). The resistivity cutoff is 50 Ωm. The assumed location of the clay cap is well resolved.

The clay cap is well resolved and within the conductivity bounds expected from a kimberlite pipe. The method presented here provides a rigorous solution allowing a more accurate fit to the data, while still being reasonably fast.

CONCLUSION

We have extended the method of HEM data interpretation based on the LQL approximation by adding a rigorous stage of inversion. The rigorous inversion iteratively updates the domain and field equations using a contraction from of the domain equation to ensure convergence. This method also includes a terrain correction, which is critical in many exploration areas. The new CEMI code LQLRigInvTOPO was carefully tested on synthetic models of HEM data and shown here with both synthetic and a field example. The new algorithm still possesses much of the speed of the original LQL inversion while providing a much more accurate result.

REFERENCES

Gribenko, A. and M. Zhdanov, 2005, Volumetric nonparametric inversion of array tensor induction logging data: Annual International Meeting, Consortium for Electromagnetic Modeling and Inversion, Expanded Abstracts, 245–262.

Hursán, G. and M. S. Zhdanov, 2002, Contraction integral equation method in three-dimensional electromagnetic modeling: Radio Sci., **37**, 1089.

Katayama, H. and M. S. Zhdanov, 2004, 3-D inversion of the helicopter-borne EM data in areas with rough topography: Annual International Meeting, Consortium for Electromagnetic Modeling and Inversion, Expanded Abstracts, 177–210.

Macnae, J. C., 1979, Kimberlites and exploration geophysics: Geophysics, **44**, 1395–1416.

Zhang, Z., 2003, 3D resistivity mapping of airborne EM data: Geophysics, **68**, 1896–1905.

Zhdanov, M. S., 2002, Geophysical inverse theory and regularization problems, volume **36** *of* Methods in Geochemistry and Geophysics: Elsevier.

Zhdanov, M. S. and S. Fang, 1996a, 3-D quasi-linear electromagnetic inversion: Radio Science, **31**, 741–754.

—— 1996b, Quasi-linear approximation in 3D EM modeling: Geophysics, **61**, 646–665.

Zhdanov, M. S. and E. Tartaras, 2002, Three-dimensional inversion of multitransmitter electromagnetic data based on the localized quasi-linear approximation: Geophys. J. Int., **148**, 506–519.

ACKNOWLEDGMENTS

The authors acknowledge the support of the University of Utah Consortium for Electromagnetic Modeling and Inversion (CEMI), which includes BAE Systems, Baker Atlas Logging Services, BGP China National Petroleum Corporation, BHP Billiton World Exploration Inc., Centre for Integrated Petroleum Research, EMGS, ENI S.p.A., ExxonMobil Upstream Research Company, INCO Exploration, Information Systems Laboratories, MTEM, Newmont Mining Co., Norsk Hydro, OHM, Petrobras, Rio Tinto - Kennecott, Rocksource, Schlumberger, Shell International Exploration and Production Inc., Statoil, Sumitomo Metal Mining Co., and Zonge Engineering and Research Organization.

We are thankful to Alex Gribenko for his contribution in the development of the iterative inversion code.